The polarization of out-of-plane scattering from microrough silicon

Thomas A. Germer and Clara C. Asmail

Optical Technology Division

National Institute of Standards and Technology

Gaithersburg, Maryland 20899

Bradley W. Scheer

VLSI Standards, Inc.

3087 North First Street

San Jose, California 95134

ABSTRACT

The polarization of light scattered by silicon having a small degree of microroughness was measured out of the plane of incidence. First-order vector perturbation theory for scattering from a rough surface predicts the behavior well. The data and theory show Brewster-like angles where $p \rightarrow p$ scattering from surface microroughness vanishes, as well as a deterministic polarization in other directions.

Optical scattering is often employed to measure microroughness levels and to detect particulate contamination on starting silicon wafers on microfabrication lines. The requirement that particles smaller than the device feature width be detected places strict demands on the sensitivity of an instrument to those particles. One important issue that limits such sensitivity is the scattering from the residual substrate microroughness. A thorough understanding of the nature of microroughness-induced scatter will allow the development of scanning surface inspection systems (SSIS) which are insensitive to microroughness and highly sensitive to other sources of scatter, such as particulate contamination and subsurface defects.

The theory of scattering from rough surfaces was developed in the past by the radar community.[1–3] Recently, those theories have been employed to interpret microroughness on the optical length scale.[4] However, experimental testing of those theories to date has been limited to measurements within the plane of incidence.[5,6] In this Letter, we present results of out-of-plane scatter measurements from a microrough silicon surface with details of the polarization of the light scattered. The results, which agree well with the theory, demonstrate the existence of Brewster-like angles for which $p \rightarrow p$ scattering vanishes. The data also demonstrate that the microroughness-induced scatter has well-defined polarization for other scattering directions.

Figure 1 shows the optical geometry of the measurement in the sample reference frame. Light from a cw laser (wavelength $\lambda = 532$ nm, TEM_{00} mode, incident power $P_i \sim 15$ mW) is incident onto the sample at an angle θ_i. Light scattered into the direction determined by a polar angle of θ_r and azimuthal (out-of-plane) angle ϕ_r is collected.

The polarization states of the incident and scattered light are defined with respect to the planes of incidence and scatter. Considering the planes of incidence and scatter as being defined by the sample normal and the incident and scatter directions, respectively, the electric field lies within that plane when it is p-polarized and perpendicular to that plane when it is s-polarized. The measurements were carried out on a goniometric optical scatter instrument which has been described elsewhere.[7] The capability for polarization selection on the incident and exitent light is performed by rotating half wave plates in conjunction with fixed polarizers.

The sample used in these measurements was a microfabricated silicon microroughness standard having a pseudorandom distribution of circular pits with nominal diameters 1.31 μm and 1.76 μm and depths 1.0 nm.[8] Use of this sample ensured that the material had a well-defined surface microroughness, with negligible particulate contamination or subsurface features. Figure 2 shows the results of measurements carried out at an incident angle of $\theta_i = 45°$ and at polar scattering angles of $\theta_r = 30°$, $45°$, and $60°$. The azimuthal angle was varied from $\phi_r = 10°$ to $\phi_r = 170°$ for each polar angle configuration. The signals for the four polarization combinations $s \to s$, $s \to p$, $p \to s$, and $p \to p$ were measured, and the results are presented normalized by the sum of all four signals.

In order to compare these results with those for microroughness-induced scatter, we summarize the results of first-order vector perturbation theory.[1−3] Assuming that the power spectral density (PSD) function of the surface height function is given by $S(\mathbf{f})$, where $\mathbf{f}$ is a two-dimensional spatial frequency in the plane of the surface, the bidirectional reflectance distribution function (BRDF) (defined as the scattered radiance normalized by the incident irradiance) is given by

$$\mathrm{BRDF} = \frac{16\pi^2}{\lambda^4} \cos\theta_i \cos\theta_r S(\mathbf{f}) \times \sum_{jk} |q_{jk} e_j e_k|^2 \tag{1}$$

where the spatial frequency vector $\mathbf{f}$ is related to θ_i, θ_r, and ϕ_r by the Bragg relations

$$\begin{aligned} \lambda f_x &= \sin\theta_r \cos\phi_r - \sin\theta_i \\ \lambda f_y &= \sin\theta_r \sin\phi_r. \end{aligned} \tag{2}$$

The e_j and e_k are the elements of the unit Jones vectors of the incident and scattered fields (in the s-p basis), respectively, and the q_{jk} are given by

$$\begin{aligned} q_{ss} &= \frac{(\epsilon-1)\cos\phi_r}{(\cos\theta_i + \sqrt{\epsilon-\sin^2\theta_i})(\cos\theta_r + \sqrt{\epsilon-\sin^2\theta_r})} \\ q_{sp} &= \frac{-(\epsilon-1)\sin\phi_r\sqrt{\epsilon-\sin^2\theta_r}}{(\cos\theta_i + \sqrt{\epsilon-\sin^2\theta_i})(\epsilon\cos\theta_r + \sqrt{\epsilon-\sin^2\theta_r})} \\ q_{ps} &= \frac{-(\epsilon-1)\sin\phi_r\sqrt{\epsilon-\sin^2\theta_i}}{(\epsilon\cos\theta_i + \sqrt{\epsilon-\sin^2\theta_i})(\cos\theta_r + \sqrt{\epsilon-\sin^2\theta_r})} \\ q_{pp} &= \frac{(\epsilon-1)\left(\epsilon\sin\theta_i\sin\theta_r - \sqrt{\epsilon-\sin^2\theta_i}\sqrt{\epsilon-\sin^2\theta_r}\cos\phi_r\right)}{(\epsilon\cos\theta_i + \sqrt{\epsilon-\sin^2\theta_i})(\epsilon\cos\theta_r + \sqrt{\epsilon-\sin^2\theta_r})}, \end{aligned} \tag{3}$$

where ϵ is the dielectric function for the material [for silicon,[9] $\epsilon(532\text{nm}) = 17.03 + 3.65i$].

By normalizing each of the polarization combinations by the sum of all the polarization combinations, the dependences on the amplitude and spatial frequency of the surface roughness, $S(\mathbf{f})$, and the wavelength of the laser are removed from the data. The solid curves in Fig. 2 represent the theoretical predictions of first-order vector perturbation theory. The agreement is excellent. Some of the deviations of the data from the theory, especially those that appear random, can be attributed to light scattered about

the room by the specularly reflected beam. Those deviations which appear systematic may be due to other scatter mechanisms being present.

The $p \to p$ scattering data show an interesting and potentially very useful behavior. The scattering from surface microroughness vanishes for certain out-of-plane angles (approximately $\phi_r = 70°$ for $\theta_r = 30°$, $\phi_r = 60°$ for $\theta_r = 45°$, and $\phi_r = 50°$ for $\theta_r = 60°$). These angles are bidirectional equivalents of Brewster's angle, where the induced dipole moment in the material is perpendicular to the plane of scatter. The usefulness of this behavior is that scattering mechanisms other than microroughness, whose signal may be otherwise masked by residual microroughness, can be detected.

We have also performed *bidirectional ellipsometry* measurements. That is, we chose a fixed incident direction, incident polarization state, and scattering direction and rotated the detection polarization analyzer to map out the polarization ellipse of the scattered light. Figure 3 shows such a measurement for $\theta_i = 45°$, $\theta_r = 45°$, $\phi_r = 90°$ and the input polarization containing equal portions of s- and p-polarized light (linearly polarized at 45°). The theoretical solid curve shows that there exists excellent agreement with the first-order vector perturbation theory. The scattering is nearly polarized linearly, although at an angle tilted with respect to the p or s axes. Although the scattering is not strictly p or s polarized, the fact that it is well defined suggests that a scattering instrument that integrates over a large portion of the entire hemisphere can be made to be microroughness-blind by appropriately choosing the detected polarization state for the corresponding scattering angle.[10]

Since different scattering sources, such as microroughness, subsurface defects, or particulate contamination, are expected to have different effects on the polarization,

bidirectional ellipsometry should allow a discrimination between different sources of scatter. Although the absolute magnitude of the BRDF has proven to be useful for analyzing scattered light, it often reflects more strongly scattering structure factors rather than form factors, and therefore is not so sensitive to the microscopic sources of scatter, as much as the correlations between them. In contrast, the polarization of scattered light will strongly indicate the paths that light follows during its trajectory, and therefore will be more sensitive to the microscopic details of the scattering process.

In summary, we have shown that first-order vector perturbation theory describes the polarization state of light scattered by a microrough silicon surface. The out-of-plane scattering shows the existence of Brewster-like angles for which $p \to p$ scattering vanishes. Furthermore, the scattering at other angles is shown to have a well defined polarization. Exploitation of this knowledge should allow a substantial increase in the detection sensitivity for particles and other defects on microrough surfaces.

FIGURE CAPTIONS

Figure 1: The optical geometry of these measurements in the reference frame of the sample.

Figure 2: The out-of-plane dependence of the polarization of scattered light from a microrough silicon sample for $\theta_i = 45^\circ$, (top) $\theta_r = 60^\circ$, (middle) $\theta_r = 45^\circ$, and (bottom) $\theta_r = 30^\circ$. The squares represent $p \to p$, the circles represent $p \to s$, the up-triangles represent $s \to p$, the down-triangles represent $s \to s$, and the curves represent the predictions of first-order vector perturbation theory. All of the data are shown normalized to the sum of all four polarization combinations.

Figure 3: A ellipsometric trace of the polarization for $\theta_i = \theta_r = 45^\circ$, $\phi_r = 90^\circ$, and the incident light polarized at 45° with respect to the plane of incidence. The solid symbols are data while the curve represents the predictions of first-order vector perturbation theory. The radial coordinate is magnitude (arbitrary units), and the angular coordinate is angle (°) from s-polarized, measured in a right-handed sense with the direction of propagation.

REFERENCES

[1] S. O. Rice, Comm. Pure and Appl. Math. **4**, 351 (1951).

[2] G. R. Valenzuela, IEEE Trans. Ant. Prop. **AP-15**, 552 (1967).

[3] D. E. Barrick, *Radar Cross Section Handbook*, (Plenum, New York, 1970).

[4] J. Elson, and J. Bennett, Opt. Eng. **18**, 116 (1979).

[5] E. Bahar, and M. A. Fitzwater, J. Opt. Soc. Am. A **2**, 2295 (1985).

[6] W. M. Bruno, J. A. Roth, P. E. Burke, W. B. Hewitt, R. E. Holmbeck, and D. G. Neal, Appl. Opt. **34**, 1229 (1995).

[7] C. C. Asmail, C. L. Cromer, J. E. Proctor, and J. J. Hsia, Proc. SPIE **2260**, 52 (1994).

[8] B. W. Scheer, Proc. SPIE **2862**, 78 (1996).

[9] E. D. Palik, *Handbook of Optical Constants of Solids*, (Academic, San Diego, 1985).

[10] T. A. Germer, and C. C. Asmail, Provisional U.S. Patent Application filed.

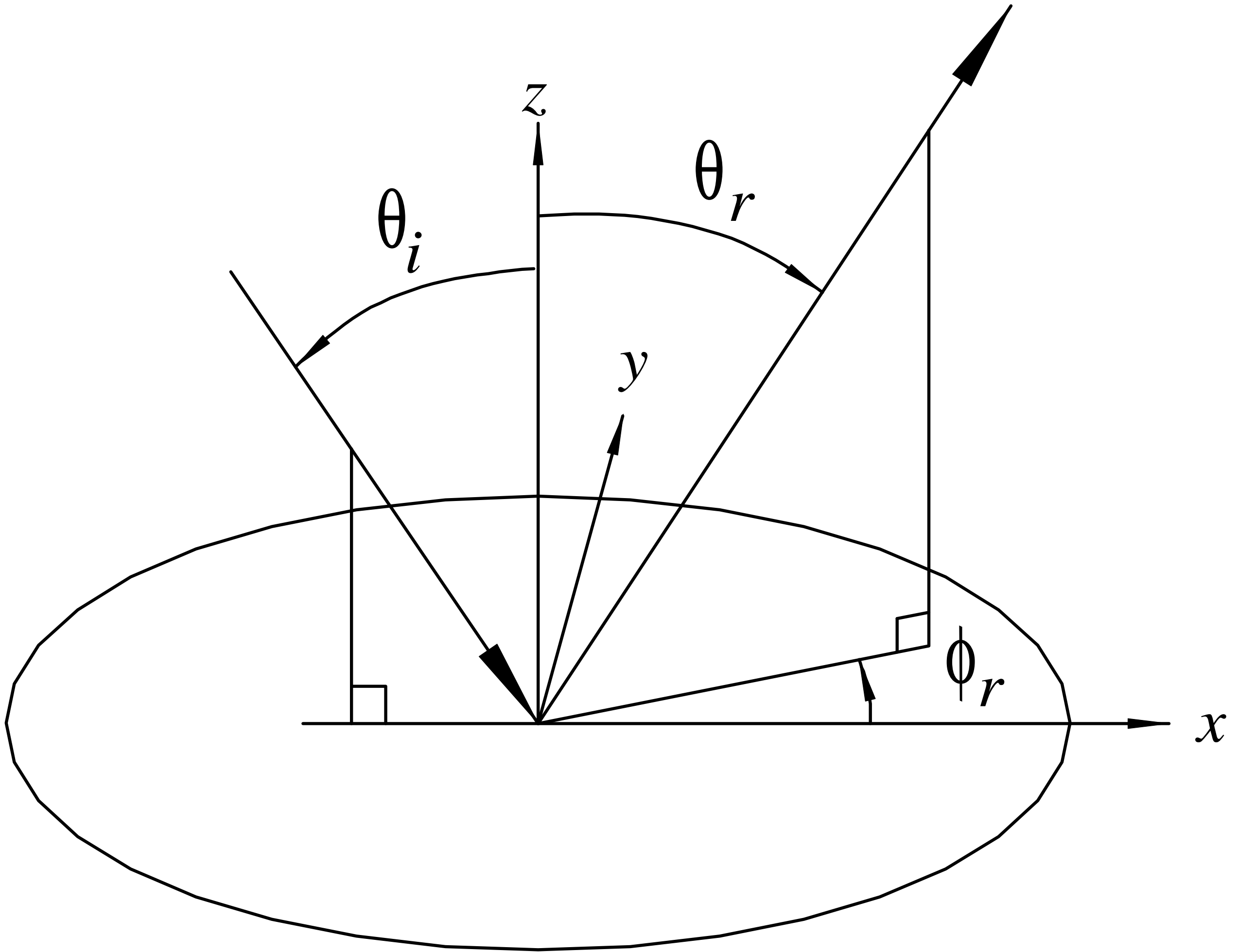

Germer, Asmail, and Scheer, Figure 1

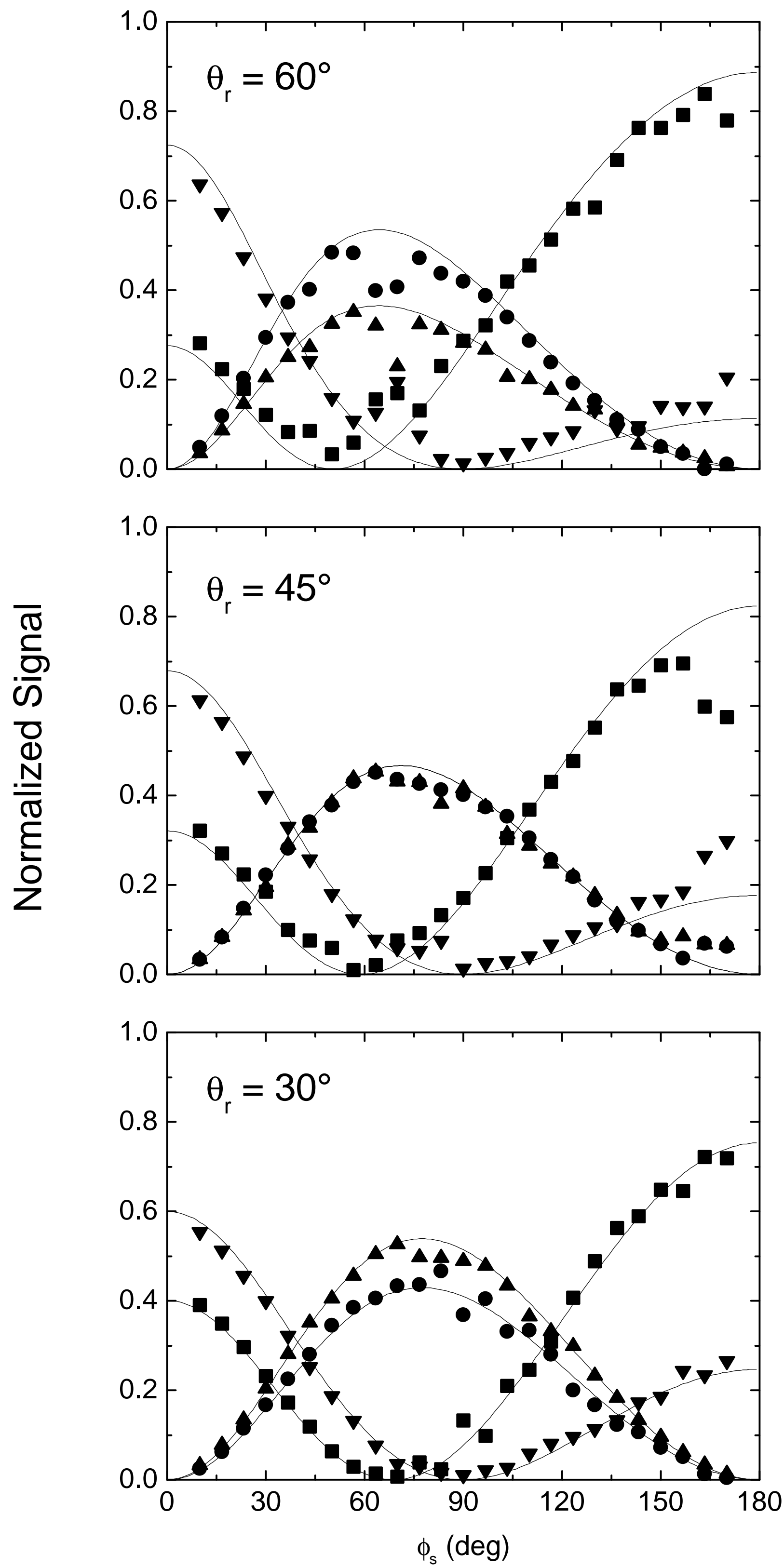

Germer, Asmail, and Scheer, Figure 2

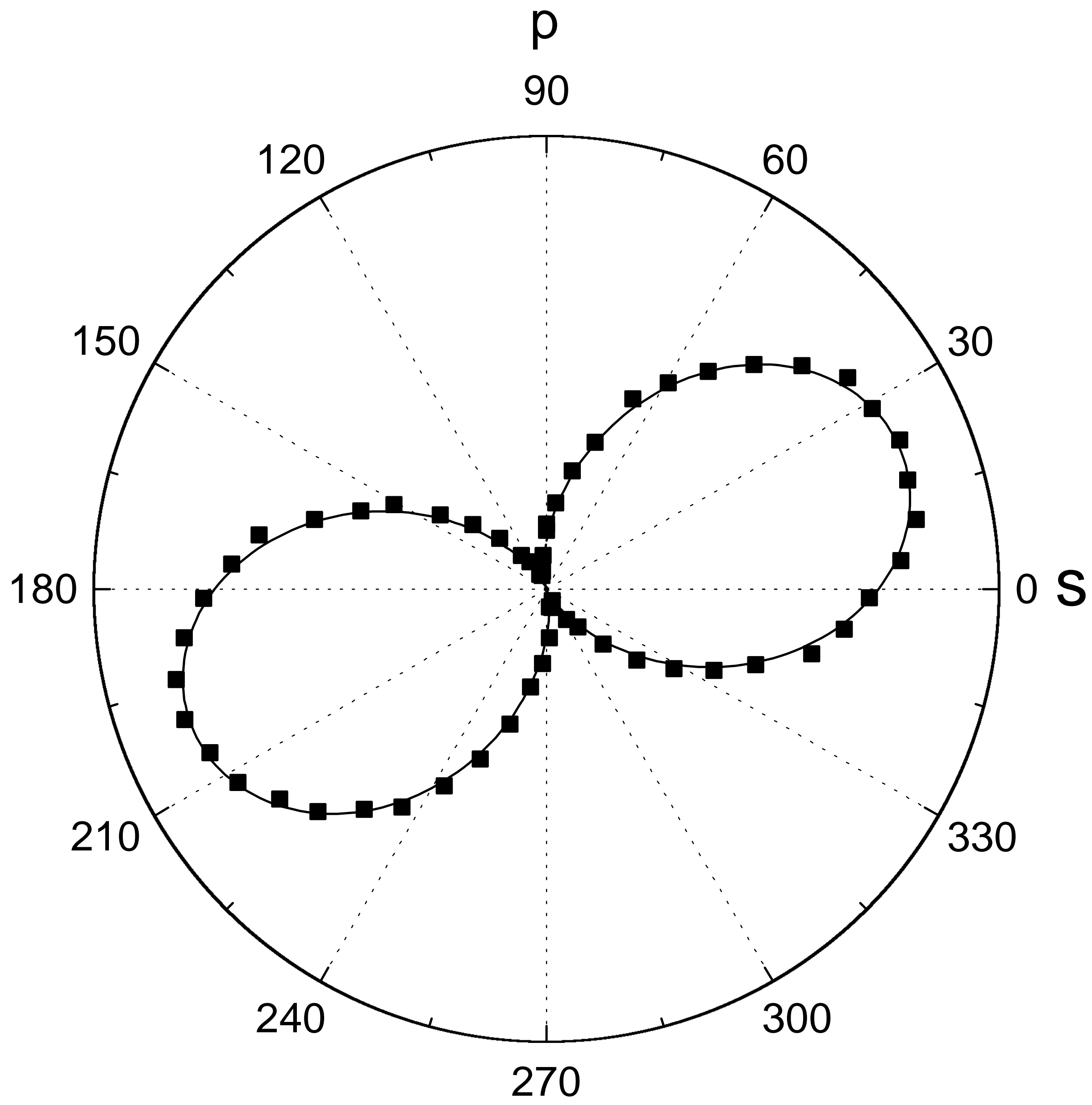

Germer, Asmail, and Scheer, Figure 3